Quantum Electronics **48** (7) 641–647 (2018)

QUANTUM CALCULATIONS

https://doi.org/10.1070/QEL16680

Effect of optical phonons on the charge qubit dynamics in a semiconductor microcavity

A.V. Tsukanov, I.Yu. Kateev

Abstract. **We consider the possibility of using optical vibrational degrees of freedom as an additional resource for controlling the evolution of a charge qubit based on a semiconductor single-electron double quantum dot. The effect of electron–photon–phonon processes on the accuracy of single-qubit operations is investigated. It is shown that, depending on the phonon decay rate and detuning of the electronic transition frequency from the optical phonon frequency, these processes can both facilitate and prevent coherent electron transfer between quantum dots.**

Keywords: *quantum computer, qubit, quantum dot, microcavity, optical phonons.*

1. Introduction

Double quantum dots (DQDs) can be considered as a system maintaning the quantum superposition of one-electron states, which are localised in each of the individual quantum dots (QDs) [1–3]. This system can be used as a charge quantum bit (qubit) with electrical [4] or optical [5] control. The QDQ properties are determined by the growth process of a semiconductor layered heterostructure (e.g., InAs/GaAs). The reliability of qubits depends on the ratio of the rates of execution of quantum gates to the rates of dissipative processes. The latter are caused by the interaction of the electron with the modes of the photon and phonon continua.

Relaxation (the spontaneous act of emission of a quantum of energy by an excited electron), which can be associated with phonons, turns out to be slow because of the so-called bottleneck effect in a QD [6]. The wave function of the electron is localised in a region with a characteristic size of about ten lattice constants, and longitudinal acoustic (LA) phonons cannot effectively interact with it because of the large difference in wavelengths. At the same time, longitudinal optical (LO) phonons have a very weak dispersion, so that the fulfilment of the law of energy conservation during relaxation requires a strictly defined transition frequency between the levels of the electron spectrum in a QD [7]. Experiments with large QD ensembles indicate the relaxation of electrons within $\sim$10 ps, accompanied by the emission of one or more phonons. This is due to a random coincidence of the transition frequencies in some QDs from the ensemble with the frequency of the optical phonon in this material. In addition to relaxation, coherent effects associated with phonons are also observed in QDs. Magnetospectroscopic studies in the far-IR region demonstrate the anticrossing of electronic levels in QDs if their energy is a multiple of the energy of an optical phonon [8]. These anticrossings point to the formation of polarons, i.e., hybridised states of the electron and phonons.

The question arises: is it possible to take advantage of the coherent coupling between a phonon and an electron for the realisation of one- and two-qubit operations? With a sufficiently large interaction coefficient and a moderate decay rate of the optical phonon, which depends on the difference in their frequencies, the phonon could play the same role as the photon in a microresonator (MR) [9, 10]. As was shown in [11], for QDs located in nanostructures, the energy of interaction of an electron with a localised optical phonon g_{LO} can be 10^{-4}–10^{-3} eV. In this case, the lifetime of a phonon can vary from several picoseconds to several nanoseconds in a broad range (of the order of several tens of milli-electron volts) of detunings [12]. The experimental proof of the possibility of using optical phonons for encoding quantum information is presented in Ref. [13], where the process of recording and reading the state of a qubit with the participation of vibrational modes of a three-dimensional diamond crystal was demonstrated for the first time.

In this paper we study the dynamics of a charge DQD-qubit with a combined photon–phonon control, taking into account the decay channels of all subsystems. We will only be interested in optical modes, so we neglect the interaction of DQDs with acoustic phonons, assuming their low density at the transition frequency between hybridised electronic states when the device operates in a low-temperature (less than 100 mK) mode. Optical phonon modes are introduced using a model of a continuous medium with free boundary conditions. This makes it possible to calculate the energy parameters of the Hamiltonian as a function of the sample size. Dependences of the populations of the logical states of the qubit (the ground DQD states) on time are found by solving the Schrödinger equation with a phenomenological account of the dissipative channels. It is shown that the probability of performing an inversion (NOT) operation in a complex manner depends on such system parameters as the detuning of the frequencies of the subsystems, the Rabi frequency, and the decay rates of the quantum states. Selecting them in a certain way, it is possible to optimise this probability, even by taking into account the imperfection of the nanostructure. A nontrivial result is the detection of the effect of self-suppression of dissipation in a DQD through a phonon channel with increasing rate of its decay.

A.V. Tsukanov, I.Yu. Kateev Institute of Physics and Technology, Russian Academy of Sciences, Nakhimovskii prosp. 34, 117218 Moscow, Russia; e-mail: ikateyev@mail.ru

Received 16 March 2018; revision received 3 May 2018
Kvantovaya Elektronika **48** (7) 641–647 (2018)
Translated by I.A. Ulitkin

2. Model and basic equations

We simulate the dynamics of a hybrid DQD–MR–phonon system by assuming a reversible energy exchange between the subsystems. If the frequencies of the phonon modes are located in the vicinity of the DQD transition frequencies and the MR frequency, then a coherent transformation of the electronic excitation of the DQD to the MR photon or to the phonons of a crystal lattice is possible. In this case, complex oscillations of the populations of the basis states of the hybrid system will be observed. Recent experiments confirm the possibility of a reversible exchange of a single quantum between a superconducting phase qubit and a phonon acoustic mode under conditions of ultralow temperatures [14].

Consider an asymmetric DQD consisting of their two separate QDs A and B (Fig. 1). Point A(B) has two single-electron states: the ground (localised) $|A(B)0\rangle$ state and the excited $|A(B)1\rangle$ state (near the edge of the potential barrier) with energies $\varepsilon_{A(B)0}$ and $\varepsilon_{A(B)1}$, respectively. We will assume that the energies of the excited states $|A1\rangle$ and $|B1\rangle$, necessary for the hybridisation of QDs due to electron tunnelling with the interaction energy V, are close. In this case, new (common for DQDs) states $|-\rangle$ and $|+\rangle$ are formed, which are linear superpositions of excited states of individual QDs. They serve as a transport channel linking QDs. The states $|A0\rangle$ and $|B0\rangle$ are not hybridised because of the absence of a tunnel coupling between them and are associated with the logical qubit states '0' and '1', i.e., $|A0\rangle \equiv |0\rangle$ and $|B0\rangle \equiv |1\rangle$. The energy difference of the ground states of the DQD is $\Delta_0 = \varepsilon_1 - \varepsilon_2$, and the splitting of the hybridised states is $\Delta_1 = \sqrt{V^2 + (\varepsilon_{A1} - \varepsilon_{B1})^2}$. The QD parameters are chosen so that the frequency $\omega_{0(1)-} = \varepsilon_- - \varepsilon_{0(1)}$ of the electronic transition $|0(1)\rangle \leftrightarrow |-\rangle$ from the ground to the lower hybridised level in the QD A(B) is close to the MR frequency ω_c (or to the frequency $\omega_{\mathrm{LO}q}$ of a set of optical phonons $q = 1 - N_{\mathrm{LO}}$), and the energy difference Δ_1 of the excited levels of the DQD is close to the frequencies $\omega_{\mathrm{LA}\,q}$ of the set $q = 1 - N_{\mathrm{LA}}$ of acoustic phonon modes. We will also consider the coupling between the acoustic phonons and the electron in the DQD to be weak, and the mode population to be low (no more than one quantum). For crystal vertical GaAs-based DQDs with the characteristic size $R = 5-10$ nm and barrier thickness $L = 10-15$ nm at a potential well depth $U = 0.2-0.3$ eV, the transition frequency is $\omega_{0(1)-} = 0.03-0.1$ eV.

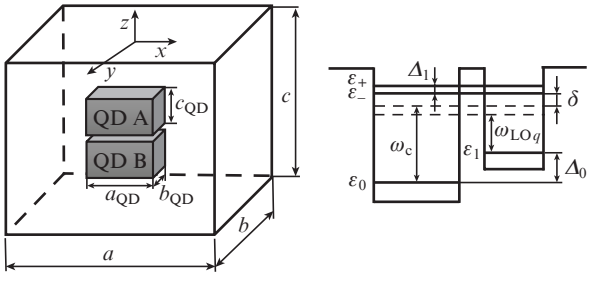

Figure 1. Schematic of a DQD in a semiconductor nanocrystal (left) and the potential profile in it (right). See notations in the text.

The Hamiltonian of isolated subsystems has the form

$$\hat{H}_0 = \sum_{k=0,1,-,+} \varepsilon_k |k\rangle\langle k| + (\omega_c - \mathrm{i}\kappa)\hat{a}^+\hat{a} + \sum_{q=1}^{N_{\mathrm{LO}}} (\omega_{\mathrm{LO}q} - \mathrm{i}\gamma_{\mathrm{LO}})\hat{b}^+_{\mathrm{LO}q}\hat{b}_{\mathrm{LO}q}, \quad (1)$$

where $\hat{a}$ is the annihilation operator for the photon in the MR; and $\hat{b}_{\mathrm{LO}q}$ is the annihilation operator of the phonon in the optical mode q. Hereinafter, the Planck constant is set equal to unity. Dissipative effects are characterised by phenomenological parameters (velocities): κ is the photon exit rate from the resonator and γ_{LO} is the decay rate of the optical phonon (here, for simplicity, it is the same for all modes). The rate of decay of phonon modes γ_{LO} is set on the basis of experimental data and varies from 10^{-6} to 10^{-9} eV [6, 7, 12]. The photon dissipation rate $\kappa \approx 10^{-5}-10^{-6}$ eV also corresponds to the observed values for high-Q semiconductor MRs [9].

The total Hamiltonian of the system can be represented in the form of the sum H_0 and the Hamiltonians of the interaction between the subsystems. The exchange of energy between the MR and DQD is described by the extended Jaynes–Cummings Hamiltonian:

$$\hat{H}_{\mathrm{JC}} = \Omega_{0-}\hat{a}\,|-\rangle\langle 0| + \Omega_{0+}\hat{a}\,|+\rangle\langle 0| + \Omega_{1-}\hat{a}\,|-\rangle\langle 1| + \Omega_{1+}\hat{a}\,|+\rangle\langle 1| + \mathrm{H.c.}, \quad (2)$$

where Ω_{0-}, Ω_{0+}, Ω_{1-} and Ω_{1+} are the coefficients of the interaction an electron in a DQD and a photon in a MR (Rabi frequencies). The latter are related to the Rabi frequencies of the optical transitions g_{Ac} and g_{Bc} of isolated QDs as follows:

$$\Omega_{0-} = \alpha g_{Ac},\ \ \Omega_{0+} = \sqrt{1-\alpha^2}\, g_{Bc},$$

$$\Omega_{1-} = \sqrt{1-\alpha^2}\, g_{Ac},\ \ \Omega_{1+} = -\alpha g_{Bc},$$

where $\alpha = \sin(\theta/2)$; and $\theta = \arctan(2V/\Delta_1)$. The estimation of the matrix elements of the optical dipole transition operator for typical values of the single-photon field amplitudes $E_c \approx 1-10$ V cm^{-1} and the radius $R \approx 5-10$ nm of the QD gives $g_{A(B)c} \approx 10^{-6}$ eV. The Hamiltonian of the interaction of an electron and optical phonons is represented by an expression analogous to (2), with the replacement of photon operators by phonon ones:

$$\hat{H}_{\mathrm{e-LO}} = \sum_{q=1}^{N_{\mathrm{LO}}} (\tilde{\Omega}_{0-}\hat{b}_{\mathrm{LO}q}\,|-\rangle\langle 0| + \tilde{\Omega}_{0+}\hat{b}_{\mathrm{LO}q}\,|+\rangle\langle 0| + \tilde{\Omega}_{1-}\hat{b}_{\mathrm{LO}q}\,|-\rangle\langle 1| + \tilde{\Omega}_{1+}\hat{b}_{\mathrm{LO}q}\,|+\rangle\langle 1|) + \mathrm{H.c.}, \quad (3)$$

and the interaction coefficients $\tilde{\Omega}_{0(1)-(+)}$ of optical phonons and electrons are calculated within the framework of a continuous medium model (see below).

The total Hamiltonian of the electron–photon–phonon system has the form

$$\hat{H} = \hat{H}_0 + \hat{H}_{\mathrm{JC}} + \hat{H}_{\mathrm{e-LO}}. \quad (4)$$

At the initial instant of time, the MR contains one photon, which is necessary for realising single-qubit rotations [9, 10]. The Schrödinger equation

$$\mathrm{i}\frac{\partial}{\partial t}|\Psi\rangle = \hat{H}\,|\Psi\rangle \quad (5)$$

specifies the evolution of the state vector $|\Psi\rangle$ of the system. This vector is represented as an expansion

$$|\Psi\rangle = \sum_{k=1}^{d} c_k |k\rangle$$

in basis vectors

$$|k\rangle = |\mathrm{i}\rangle_{\mathrm{DQD}} \otimes |n_\mathrm{c}\rangle \otimes \prod_{q=1}^{N_\mathrm{LO}} |n_q\rangle, \quad k = 1 - d,$$

where $d = 2(N_\mathrm{LO} + 1)$, taking into account the conditions $n_\mathrm{c} = 0, 1$ and $n_q = 0, 1$. It is convenient to pass to the frame of reference associated with the MR, using a unitary transformation

$$\hat{T} = \exp\left[-\mathrm{i}\omega_\mathrm{c}\left(|-\rangle\langle -| + |+\rangle\langle +| + \hat{a}^+\hat{a} + \sum_{q=1}^{N_\mathrm{LO}} \hat{b}^+_{\mathrm{LO}q}\hat{b}_{\mathrm{LO}q}\right)t\right]; \quad (6)$$

in this case, the Hamiltonian $\hat{H}_0$ acquires the form

$$\hat{\tilde{H}}_0 = \hat{T}^+\hat{H}_0\hat{T} + \mathrm{i}\frac{\partial \hat{T}^+}{\partial t}\hat{T} = \Delta_0 |1\rangle\langle 1| + \delta|-\rangle\langle -|$$

$$+ (\delta + \Delta_1)|+\rangle\langle +| - \mathrm{i}\kappa\hat{a}^+\hat{a} + \sum_{q=1}^{N_\mathrm{LO}} (\Delta_{\mathrm{LO}q} - \mathrm{i}\gamma_\mathrm{LO})\hat{b}^+_{\mathrm{LO}q}\hat{b}_{\mathrm{LO}q}, \quad (7)$$

and expressions (2) and (3) do not change. Here, $\delta = \omega_{0-} - \omega_\mathrm{c}$ is the detuning of the MR frequencies and the transition $|0\rangle \leftrightarrow |-\rangle$ in the DQD, and $\Delta_{\mathrm{LO}q} = \omega_{\mathrm{LO}q} - \omega_\mathrm{c}$ is the detuning of the MR frequencies and the optical phonon mode q.

In the next section, we present the calculation of the interaction coefficient of an electron with localised optical phonons for several variants of the DQD position in a crystal.

3. Interaction of QDs with localised optical phonons

In crystals of small size (nanocrystals), phonons inevitably experience an effect of dimensional confinement. This phenomenon is somewhat similar to the effect of electron localisation in a quantum well. The boundary conditions lead to the same restrictions as in the case of an electron in the phase space imposed on the phonon wave vector $\boldsymbol{q}$. Therefore, this effect will affect the interaction of phonons both with each other and with charge carriers. Following [11], we consider a single semiconductor QD placed in a GaAs crystal of size $a \times b \times c$. In the absence of an external pressure, the vector $\boldsymbol{u}(\boldsymbol{r})$ of displacement of long-wavelength optical phonons in a crystal is represented in the form

$$\boldsymbol{u}(x, y, z) = \nabla\Phi(x, y, z),$$

$$\Phi(x, y, z) \propto \sin q_x x \sin q_y y \sin q_z z,$$

where

$$q_x = \frac{\pi}{a}n_1, \quad q_y = \frac{\pi}{b}n_2, \quad q_z = \frac{\pi}{c}n_3$$

are the projections of the phonon wave vector onto the corresponding coordinate axes; and $n_{1,2,3} = 1, 2, 3, \ldots$. The Hamiltonian of the interaction of electrons and optical phonons in a QD can be represented as follows [11]:

$$\hat{H}_{\mathrm{e-ph}} = \sum_q V_q \sin q_x x \sin q_y y \sin q_z z (\hat{b}_{\mathrm{LO}q} + \hat{b}^+_{\mathrm{LO}q}), \quad (8)$$

where

$$V_q^2 = \frac{16\pi e^2\omega_{\mathrm{LO}q}}{q^2 abc}\left(\frac{1}{\varepsilon_\infty} - \frac{1}{\varepsilon_0}\right); \quad q^2 = q_x^2 + q_y^2 + q_z^2; \quad (9)$$

$\varepsilon_{0(\infty)}$ is the static (high-frequency) dielectric constant of the crystal material; and e is the electron charge. Let us consider the transition of an electron in a single QD from the excited state $|e\rangle$ to the ground state $|g\rangle$, accompanied by the excitation of optical phonons. The expression for the phonon interaction coefficient with the wave vector $\boldsymbol{q}$ and QD for this process has the form

$$g_{\mathrm{LO}q} = \langle g, n_q + 1 | \hat{H}_{\mathrm{e-ph}} | e, n_q \rangle, \quad (10)$$

where n_q is the number of phonons in the state q. Under the assumption of infinitely high potential walls for an electron in the conduction band of a QD in the form of a rectangular parallelepiped with sides a_QD, b_QD and c_QD,

$$g_{\mathrm{LO}q} = \sqrt{n_q + 1}\, V_q I_x I_y I_z. \quad (11)$$

Here, I_x, I_y and I_z are the dimensionless overlap integrals along the corresponding coordinate axes. If the conditions

$$a = \frac{a_\mathrm{QD} n_1}{2m_1 - 1}, \quad b = \frac{b_\mathrm{QD} n_2}{2m_2}, \quad c = \frac{c_\mathrm{QD} n_3}{2m_3} \quad (12)$$

are met, where $m_{1,2,3}$ are positive integers, these integrals will be zero, and consequently $g_{\mathrm{LO}q} \equiv 0$. If the size of the crystal is much larger than that of the QD, i.e., $a \gg a_\mathrm{QD}$ ($b \gg b_\mathrm{QD}$, $c \gg c_\mathrm{QD}$), then the integrals in (11) take the form:

$$I_x = -\frac{16n_1}{9\pi}\frac{a_\mathrm{QD}^2}{a^2}, \quad I_y = \frac{\pi n_2}{2}\frac{b_\mathrm{QD}^2}{b^2}, \quad I_z = \frac{\pi n_3}{2}\frac{c_\mathrm{QD}^2}{c^2}. \quad (13)$$

This means that the interaction energy $|g_{\mathrm{LO}q}|$ decreases rapidly with increasing volume.

We calculated the $g_{\mathrm{LO}q}$ for a QD embedded in a GaAs crystal for various sizes of the QD and the crystal. The energy of the optical phonon $\omega_{\mathrm{LO}q}$ was assumed to be ~36 meV. The static (ε_0) and high-frequency (ε_∞) dielectric constants of GaAs were 13.2 and 10.9, respectively [15]. We have neglected the effects associated with the reflection of phonons from the interfaces between the materials of the QD and the crystal.

Let us examine the interaction of a cubic QD and phonons in a cubic nanocrystal, i.e., we set $b = c = a$ and $b_\mathrm{QD} = c_\mathrm{QD} = a_\mathrm{QD}$. First we consider the case when the size of the QD coincides with that of the nanocrystal: $a_\mathrm{QD} = a$. If n_1 is an odd number, then the integral I_x is strictly equal to zero, and vice versa, $I_y = 0$ and $I_z = 0$ for even n_2 and n_3. This means that the QD does not interact with such phonons. For even n_1 and odd $n_{2,3}$, the overlap integrals take the form:

$$I_x = -\frac{16n_1}{\pi(n_1 - 1)(n_1 + 1)(n_1 - 3)(n_1 + 3)}, \quad n_1 = 2, 4, \ldots,$$

$$I_{y,z} = -\frac{8}{\pi n_{2,3}(n_{2,3} - 2)(n_{2,3} + 2)}, \quad n_{2,3} = 1, 3, \ldots. \quad (14)$$

Thus, for any phonon, the overlap integrals do not depend on the size of the nanocrystal, and the interaction energy $|g_{\mathrm{LO}q}|$ is determined only by the value of V_q and, according to formulas (9) and (11), is $\sim 1/\sqrt{a}$. If we compare the values of $|g_{\mathrm{LO}q}|$ for phonons with different $\boldsymbol{q}$, then it turns out that the interaction energy is maximal for a phonon with $n_1 = 2$, $n_2 = 1$, $n_3 = 1$

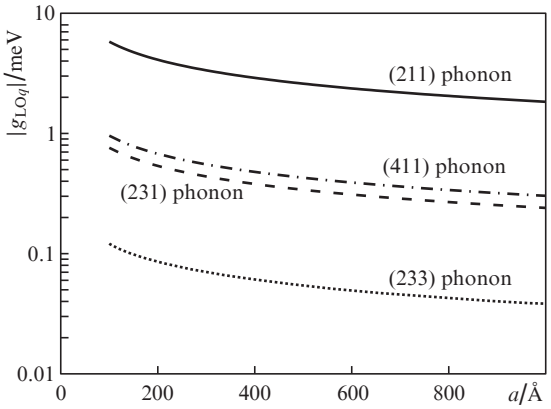

Figure 2. Dependences of the interaction energy $|g_{LOq}|$ on the cubic nanocrystal size a for different quantum numbers.

[(211) phonon], since the quantities $|I_{x,y,z}|$ decrease with increasing $n_{1,2,3}$ (Fig. 2). For example, for $a = 100$ Å, we have $|g_{LOq}| = 5.8$ meV for the (211) phonon and 0.8 meV for the (231) phonon.

Now we consider the case when the characteristic size of a cubic nanocrystal exceeds the size of a QD: $a > a_{QD}$. Then all phonons will interact with the QD, because there are no $n_{1,2,3}$ for which the values of $I_{x,y,z}$ would be strictly zero for any a and a_{QD}. For $a = a_{QD}$, the interaction energy is nonzero only for even n_1 and simultaneously for odd $n_{2,3}$, and in the remaining cases $g_{LOq}(a = a_{QD}) \equiv 0$. As a increases, the value of $|g_{LOq}|$ first increases (Figs 3a, 3c and 3d), except for the case corresponding to the (211) phonon (Fig. 3b), and then maxima are observed, the number of which is determined by the quantum numbers $n_{1,2,3}$ (Figs 3b and 3d). For some values of a corresponding to expressions (12), $g_{LOq} = 0$. Note that only for the (211) phonon the quantity $|g_{LOq}|$ decreases at $a \geqslant a_{QD}$. For $a \gg a_{QD}$, according to Eqn (13), the interaction energy decreases monotonically, and for a QD of a smaller size, a weaker interaction with phonons is observed.

Consider a cubic QD placed in a thin GaAs plate, for which the following relationships are satisfied: $a_{QD} < a \ll b$, c. Then, the interaction of QDs with the plate will be determined only by the overlap integral I_x and by n_1, since the integrals I_y and I_z do not depend on the plate thickness a and, consequently, the numbers $n_{2,3}$ will not have a significant effect on g_{LOq}. We have calculated the energy of interaction of QDs and phonons in a plate of size $b \times c = 3000 \times 3000$ Å. The main difference in the behaviour of g_{LOq} in comparison with the case of a cubic nanocrystal (Fig. 3) is that for the plate (Fig. 4), the growth of $|g_{LOq}|$ with an increase in the QD size in the limit $a \gg a_{QD}$ is much more noticeable. It should be emphasised, however, that the energy of the interaction between the QD and phonons in the plate is two orders of magnitude smaller than that in the nanocrystal, which is associated with a decrease in the overlap integrals $I_{y,z}$ and the value of V_q (9) with an increase in the plate area.

4. Dynamics of a charge qubit in the photon and mechanical single-quantum fields

To realize single-qubit rotations using optical fields in a DQD consisting of two QDs with similar spectral properties, it is sufficient to use monochromatic laser radiation [5] or single-mode laser radiation [9]. If QD parameters are different and

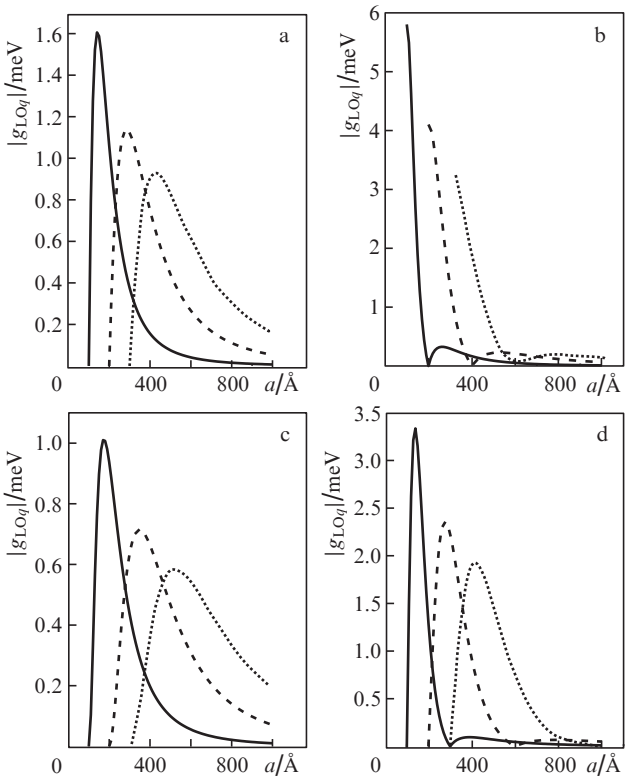

Figure 3. Dependences of the interaction energy $|g_{LOq}|$ on the cubic nanocrystal size a for (a) the (111) phonon, (b) (211) phonon, (c) (121) phonon and (d) (311) phonon at a_{QD} = (solid curves) 100, (dashed curves) 200 and (dotted curves) 300 Å.

the DQD is asymmetric, an additional source of electromagnetic field (second laser or MR) is required. In this case, each field generates an optical transition in one of the QDs. As a result, a three-level scheme is formed for transferring an electron from the ground (localised) state in one QD to the ground state in another QD via an excited (delocalised) state in the DQD. The transfer is accompanied by entanglement of the electronic and photon degrees of freedom, which can be used to perform two-qubit operations, in which the photon plays the role of a carrier of interaction between remote DQDs (transport qubit) [9, 10]. If the photon field is replaced by a phonon field, then a delocalised mechanical oscillation (optical phonon) can be used as a transport qubit. We have already mentioned above the weak dispersion of optical vibrational modes. Therefore, in the calculations we assume that the phonon frequency is N_{LO} times degenerate, i.e., $\omega_{LOq} \equiv \omega_{LO}$ for all modes, and we will henceforth omit the mode index. In addition, we assume that the interaction coefficients A and B of the QD with the MR are the same: $g_{Ac} = g_{Bc} \equiv g_c$.

We assume that the vibrations of the crystal lattice, represented in the form of a quantum field, are able to maintain coherence for a certain period of time. Then the crystal can be used to store optical qubits (photons), i.e., as a quantum memory. The experiment performed by Lee et al. [13] confirms the possibility of recording/reading quantum information in the form of nonclassical vibrational states using Raman scattering at room temperature. The three-level scheme, which includes the ground state of a diamond crystal without a phonon and with a phonon, as well as a virtually populated excited state (exciton), allows the photon of a laser

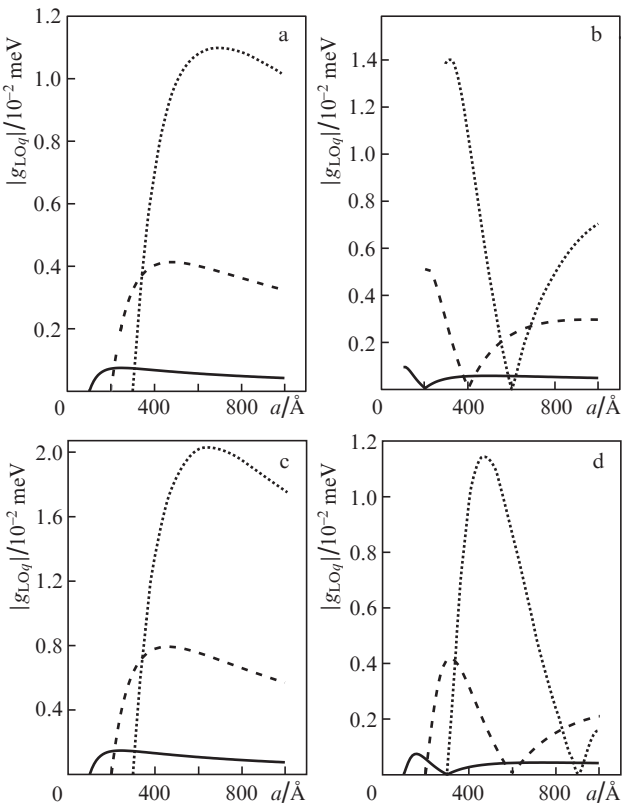

Figure 4. Dependences of the interaction energy $|g_{LOq}|$ on the plate thickness a for (a) the (111) phonon, (b) (211) phonon, (c) (121) phonon and (d) (311) phonon at a_{QD} = (solid curves) 100, (dashed curves) 200 and (dotted curves) 300 Å.

(qubit) to be reversibly transformed into an optical phonon at a frequency of 40 THz and into a signal photon in the focusing region of laser fields. Despite the very low probability of successful recording (10%) and reading (0.1%), as well as a short phonon lifetime (less than 7 ps), the study of the statistical properties of signal photons accompanying the creation/annihilation of a phonon indicates the coherent nature of the lattice vibration.

It is assumed that in the scheme presented below, a complete transformation of the optical quantum into the vibrational quantum and back occurs in the course of electron transfer to the DQD. We choose as initial the state in which the DQD is in the logical state '0', the MR contains one photon, and the optical phonon reservoir is in the vacuum state. In this case, the conditions of strict electron–photon–phonon resonance are satisfied: $\delta = 0$ and $\Delta_{LO} = \Delta_0$. Let us present the simulation results for two decay rates of an optical phonon (Fig. 5). It is easy to see that the accuracy of the NOT operation is determined (with other conditions satisfied) by the maximum decay rate.

It follows from calculations of the electron–phonon interaction coefficients that they can differ significantly from the coefficients of the electron–photon interaction. In this case, the successful implementation of the gates assumes the equality of these coefficients. Is it possible in the general case to compensate for their difference by varying any of the parameters of the Hamiltonian, for example, the frequency of one of the transitions? Let us consider the dependence of the maximum probability P_1 of electron transfer between QDs on the energy difference of the excited Δ_1 levels (Fig. 6). It is seen

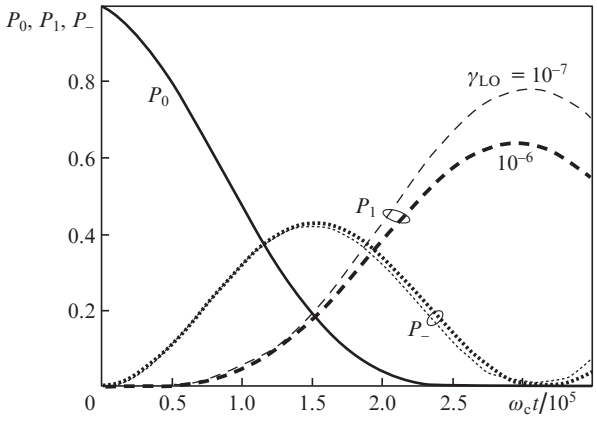

Figure 5. Dependences of the population of states in the DQD (P_0, P_1, P_-) on time for the decay rates of the optical phonon γ_{LO} = (thin curves) 10^{-7} and (thick curves) 10^{-6}. Parameters of the system (in units of frequency ω_c of the MR mode) are as follows: $g_c = 10^{-5}$, $g_{LO} = 10^{-5}$, $\Delta_0 = -10^{-1}$, $\Delta_1 = 0$, $V = 10^{-2}$, $\kappa = 10^{-6}$.

that at $g_c = g_{LO}$ the curve has a maximum at exact coincidence of energies. If $g_c \neq g_{LO}$, then the maximum value can be restored by the relative bias of energies ε_{A1} and ε_{B1} in an external electric field. This approach is effective when g_c and g_{LO} differ by no more than twofold.

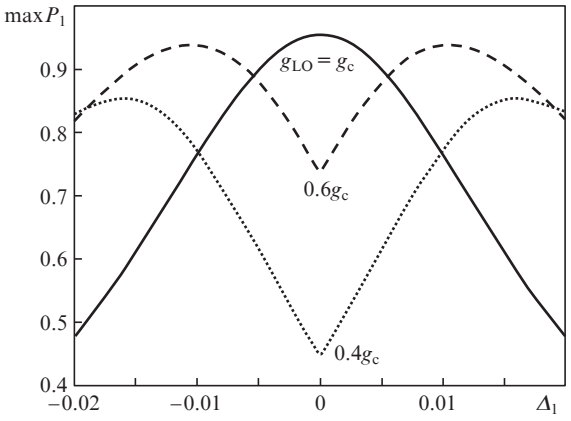

Figure 6. Dependences of the maximum probability P_1 of electron transfer between the qubit's logical states on the parameter Δ_1 for different g_{LO}. Parameters of the system (in units of frequency ω_c of the MR mode) are as follows: $g_c = 10^{-5}$, $\Delta_0 = -10^{-1}$, $\kappa = 10^{-6}$.

As is well known, in three-dimensional crystals the optical phonon modes are virtually degenerate in frequency. In nanostructures with a lower dimensionality, their spectrum has a quasi-discrete structure that allows the selection of several (and even one) modes as a qubit control element (see Section 3). However, an increase in the number of working modes with different interaction coefficients can lead to an imbalance in the Rabi frequencies and desynchronisation of population oscillations in the DQD. Figure 7 shows the dependence of the maximum probability of transfer from state 0 to state 1 on the number N_{LO} of phonon modes for several cases. If we assume that the optical modes are independent, the addition of a new mode with the same interaction coefficient leads to an increase in the integral Rabi fre-

quency during the interaction of the DQD with phonons. This causes a sharp decrease in the probability of transfer (solid curve). Thus, as the number of modes increases, it is necessary to adjust (increase) the coefficients of the interaction of the DQD with the MR. The growth of N_{LO} can be associated with an increase in the size of the structure, while the amplitudes of mechanical oscillations and, consequently, the Rabi frequency of individual modes will decrease. The dashed curve reflects the dependence of $\max P_1$ on N_{LO} for $g_{LO} = g_{0LO}/N_{LO}$ and also shows a decrease in the probability of transfer. If we assume that the modes interact, this leads to their hybridisation and the formation of a new basis. When the initial Rabi frequencies of the individual modes are equal, this is accompanied by the appearance of the factor $\sqrt{N_{LO}}$ in the expression for the integral Rabi frequency. Thus, to compensate for this imbalance, it is necessary that the partial Rabi frequencies decrease in proportion to $1/\sqrt{N_{LO}}$. In this case, the magnitude of the maximum does not depend on N_{LO} and is determined by the single-mode regime parameters (dashed line).

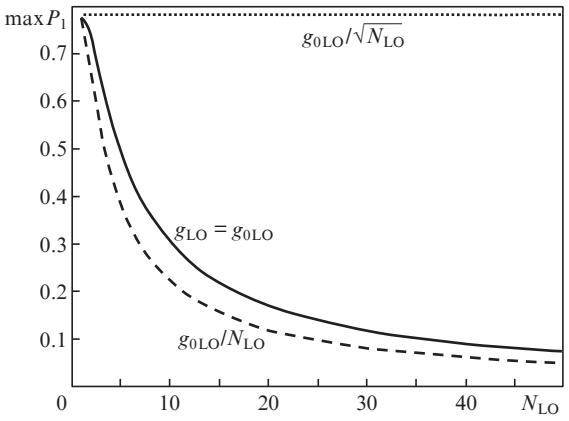

Figure 7. Dependences of the maximum probability P_1 of electron transfer between the qubit's logical states on the number N_{LO} of modes for different g_{LO}. Parameters of the system (in units of frequency ω_c of the MR mode) are as follows: $\Delta_0 = -10^{-1}$, $\Delta_1 = 0$, $V = 10^{-2}$, $g_c = 10^{-5}$, $\kappa = 10^{-7}$, $\gamma_{LO} = 10^{-6}$.

Let us return to the DQD qubit with monochromatic control. In this case, the symmetric DQD will experience the action of the single-photon field of the MR, and will also interact with the optical vibrational modes. Both sources can act as independent generators of single-qubit evolution and at the same time represent channels of loss of coherence. Let us show how serious can be the influence of phonon modes with a short lifetime interacting with the DQD on the accuracy of operations in the single-photon MR regime. Figure 8 shows the curves that illustrate the dependence of $\max P_1$ on the decay rate of the phonon mode γ_{LO} for several values of detuning Δ_{LO} and $N_{LO} = 1$. First of all, we note that if the frequencies of the DQD, MR, and optical phonon coincide exactly, the quantum evolution of the qubit will differ from that described by a resonant three-level scheme. The principle possibility of the DQD inverting is retained only if the initial state of the MR – optical phonon subsystem is an equilibrium superposition of their excited states. If, at the initial instant of time, only the MR mode contains one photon, oscillations that generate a correct one-qubit operation will be superimposed by oscillations caused by the redistribution of energy between the photon and phonon modes via the DQD. As a result, the maximum probability of inversion of the qubit, even at a low dissipation rate, does not exceed 0.5. To reduce this effect, it is necessary to choose the DQD transition frequency different from that of the optical mode. It can be seen (Fig. 8) that if the detuning Δ_{LO} turns out to be much larger than the Rabi frequency g_{LO}, then the effect of the phonon mode on the accuracy of single-qubit rotations decreases. This is due to the suppression of photon – phonon hybridisation with increasing detuning of the mode frequencies.

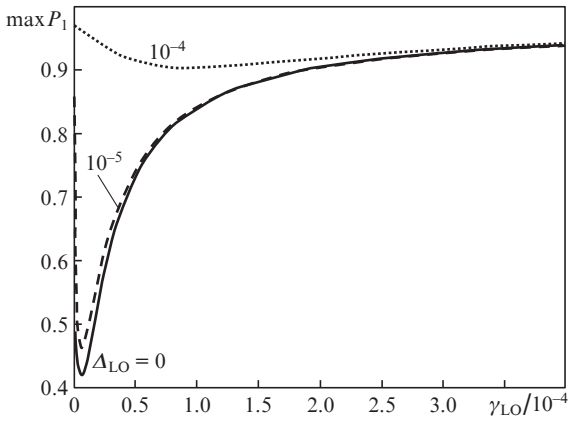

Figure 8. Dependences of the maximum probability P_1 of electron transfer between the qubit's logical states on the decay rate γ_{LO} of the phonon mode for various detunings Δ_{LO}. Parameters of the system (in units of frequency ω_c of the MR mode) are as follows: $\Delta_0 = 0$, $\Delta_1 = 0$, $V = 10^{-2}$, $g_c = 10^{-5}$, $g_{LO} = 10^{-5}$, $\kappa = 10^{-7}$.

Analysis of the dependences reveals one interesting feature. An increase in the decay rate γ_{LO} of the phonon mode in the range from 10^{-7} to 10^{-5}, which means an increase in the dissipative effect on the qubit, is accompanied by a decrease in the value of $\max P_1$. However, starting with the values $\gamma_{LO} \approx 10^{-5}$, a rapid growth of $\max P_1$ is observed with attaining an asymptotic value common for all detunings. It corresponds to the case when the interaction with the phonon mode is completely absent, and the deviation of the maximum of the transfer probability from unity is due exclusively to the dissipation of photons from the MR. Such an unusual, at first glance, result can be explained as follows. It is known that the dissipation rates, like the difference in the Rabi frequencies for electronic transitions in individual QDs, affect the effective tuning of the frequencies of the subsystems. Consequently, with increasing parameters κ and γ_{LO}, the detuning of the frequencies of the photon and phonon modes from the frequency of the transition to the DQD also increase, which leads to blocking of the decay channel by the source of dissipation. Further investigation of this extremely interesting and practically important effect will be carried out elsewhere using a more rigorous model based on the Lindblad equation.

5. Conclusions

We have considered a scheme for the combined control of the charge DQD qubit using single-quantum optical and mechanical fields. An analysis of the population dynamics of the system within the framework of the Schrödinger phenomenological model reveales a number of features that reflect the

complex interaction of the electron, photon, and phonon subsystems. In particular, the optical phonon mode of the nanostructure can act as an analogue of the photon MR mode in controlling the qubit on the basis of an asymmetric DQD, if the rate of the mode decay is small. In this case, the presence or absence of a quantum in the photon or phonon mode is uniquely associated with the implementation of the NOT gate in the DQD, which can be used to entangle several distant DQD qubits, and also to create elements of quantum memory. If the decay rate is high (in comparison with the interaction coefficients of the DQD and the mode), the imbalance of effective detunings results in the blocking of the outflow of energy from the system. This makes it possible to apply a symmetrical scheme with the control of the evolution of the state in the DQD by the MR field in both resonant and Raman variants.

As a concrete example, the interaction coefficients of localised optical phonons and electrons in a cubic QD embedded in a cubic GaAs nanocrystal have been calculated. It has turned out that the dependence of the interaction energy of optical phonons with the QD on the crystal size has several maxima associated with the effect of phonon localisation. In addition, for each phonon, it is possible to select the size of the nanocrystal so that its interaction with the QD is absent. We have demonstrated that for crystals of large size, the interaction energy increases with increasing QD size. Similar properties are also observed for QDs embedded in a thin GaAs plate, but in this case the interaction of QDs and optical phonons is much weaker.

The improvement of the charge qubit control schemes based on the described principle implies an increase in the lifetimes of a photon in the MR and a phonon by engineering the optical and mechanical properties of the nanostructure containing qubits. As shown by experiments, there are several approaches related to the development of design and improvement of the technology of manufacturing of such systems.

It should be noted that quantum operations in two-level systems, realised by phonon emission/absorption, are being investigated in many theoretical works (see, for example, [16–18]). It was shown in [16] that the increase in the energy of the electron–phonon interaction leads to a decrease in the electron transition time between the levels in the quantum wire and, consequently, to an increase in the rate of quantum operations. On the other hand, increasing the speed of operations can be achieved, in particular, by modifying the phonon spectrum, which consists in placing a quantum emitter in a phonon resonator and optimising the design of the latter by tuning the frequency of one of its modes to resonance with the frequency of the electronic transition between the emitter levels [17]. In this case, there is a phenomenon similar to the Purcell effect [19]. In our approach, the evolution of the DQD qubit is controlled both by the mechanical field of the localised optical phonon and by the electromagnetic field of the photon in the MR. This makes it possible to more effectively control the evolution of the qubit by selecting appropriate frequency detunings for the mechanical and optical subsystems.

Acknowledgements. The work was carried out within the framework of the State Task of the Federal Agency for Scientific Organisations of Russia.

References

1. Hayashi T., Fujisawa T., Cheong H.D., Jeong Y.H., Hirayama Y. *Phys. Rev. Lett*., **91**, 226804 (2003).
2. Fedichkin L., Yanchenko M., Valiev K.A. *Nanotechnology*, **11**, 387 (2000).
3. Li X.-Q., Arakawa Y. *Phys. Rev. A*, **63**, 012302 (2000).
4. Tsukanov A.V., Valiev K.A. *Microelektron*., **36**, 83 (2006).
5. Tsukanov A.V., Openov L.A. *Semiconductors*, **38**, 91 (2004) [*Fiz. Tekh. Poluprovodn*., **38**, 94 (2004)].
6. Urayama J., Norris T.B. *Phys. Rev. Lett*., **86**, 4930 (2001).
7. Grange T., Ferreira R., Bastard G. *Phys. Rev. B*, **76**, 241304 (2007).
8. Hameau S., Isaia J.N., Guldner Y., Deleporte E., Verzelen O., Ferreira R., Bastard G., Zeman J., Gérard J.M. *Phys. Rev. B*, **65**, 085316 (2002).
9. Tsukanov A.V. *Phys. Rev. A*, **85**, 012331 (2012).
10. Tsukanov A.V., Kateev I.Yu. *Microelektron*., **42**, 246 (2013).
11. Li X.-Q., Nakayama H., Arakawa Y. *Phys. Rev. B*, **59**, 5069 (1999).
12. Zibik E.A., Grange T., Carpenter B.A., Porter N.E., Ferreira R., Bastard G., Stehr D., Winnerl S., Helm M., Liu H.Y., Skolnick M.S., Wilson L.R. *Nature Mat*., **8**, 803 (2009).
13. Lee K.C., Sussman B.J., Sprague M.R., Michelberger P., Reim K.F., Nunn J., Langford N.K., Bustard P.J., Jaksch D., Walmsley I.A. *Nat. Photonics*, **6**, 41 (2012).
14. O'Connell A.D., Hofheinz M., Ansmann M., Bialczak R.C., Lenander M., Lucero E., Neeley M., Sank D., Wang H., Weides M., Wenner J., Martinis J.M., Cleland A.N. *Nature*, **464**, 697 (2010).
15. Jacak L., Machnikowski P., Krasnyj J., Zoller P. *Europhys. J. D*, **22**, 319 (2003).
16. Wang C.-T., Wu Z.-Y., Zhao C.-L., Ding Z.-H., Xiao J.-L. *Chin. Phys. B*, **21**, 057108 (2012).
17. Reinke C.M., El-Kady I. *AIP Adv*., **6**, 122002 (2016).
18. Pouthier V. *J. Chem. Phys*., **139**, 054103 (2013).
19. Purcell E.M. *Phys. Rev*., **69**, 681 (1946).